Acta Crystallographica Section B
Structural Science
ISSN 0108-7681

Symmetrically 4,6-disubstituted 2-aminopyrimidines and 2-amino-5-nitrosopyrimidines: interplay of molecular, molecular–electronic and supramolecular structures

Antonio Quesada,[a,b] Antonio Marchal,[a] Manuel Melguizo,[a] John N. Low[b,c] and Christopher Glidewell[d]*

[a]Departamento de Química Inorgánica y Orgánica, Universidad de Jaén, 23071 Jaén, Spain, [b]School of Engineering, University of Dundee, Dundee DD1 4HN, Scotland, [c]Department of Chemistry, University of Aberdeen, Meston Walk, Old Aberdeen AB24 3UE, Scotland, and [d]School of Chemistry, University of St Andrews, St Andrews KY16 9ST, Scotland

Correspondence e-mail: cg@st-andrews.ac.uk

Received 30 September 2003
Accepted 29 October 2003

The structures of six symmetrically 4,6-disubstituted 2-aminopyrimidines, four of them containing a 5-nitroso substituent, have been determined. The nitroso compounds, in particular, exhibit polarized molecular–electronic structures leading to extensive charge-assisted hydrogen bonding. The intermolecular interactions observed include hard hydrogen bonds of N—H···N and N—H···O types together with O—H···O and O—H···N types in 2-amino-4,6-bis(2-hydroxyethylamino)-5-nitrosopyrimidine; soft hydrogen bonds of the C—H···O type in both 2-amino-4,6-bis(morpholino)-5-nitrosopyrimidine (3) and 2-amino-4,6-bis(benzylamino)-5-nitrosopyrimidine (4), and of the C—H···π(arene) type in both 2-amino-4,6-bis(piperidino)pyrimidine (1) and 2-amino-5-nitroso-4,6-bis(3-pyridylmethoxy)pyrimidine (5); and aromatic $\pi\cdots\pi$ stacking interactions in 2-amino-5-nitroso-4,6-bis(3-pyridylmethoxy)pyrimidine. The supramolecular structures formed by the hard hydrogen bonds are finite, zero-dimensional in (1), one-dimensional in 2-amino-4,6-bis(3-pyridylmethoxy)pyrimidine (2), two-dimensional in both (3) and (4), and three-dimensional in both (5) and 2-amino-4,6-bis(2-hydroxyethylamino)-5-nitrosopyrimidine.

1. Introduction

We have recently reported the interplay of molecular, molecular–electronic and supramolecular structures in a wide range of amino-substituted O^6-benzyl-5-nitrosopyrimidines (Quesada, Marchal *et al.*, 2002; Melguizo *et al.*, 2003); however, the compounds studied in the earlier work generally contained two different substituents in the 2 and 4 positions. Continuing with the development of that work we now present a study of the molecular and supramolecular structures of a range of symmetrically 4,6-disubstituted 2-aminopyrimidines, some of which carry a 5-nitroso substituent and some of which do not, namely 2-amino-4,6-bis(piperidino)pyrimidine [(1); see Scheme (I)], 2-amino-4,6-bis(3-pyridylmethoxy)pyrimidine (2), 2-amino-4,6-bis(morpholino)-5-nitrosopyrimidine (3), 2-amino-4,6-bis(benzylamino)-5-nitrosopyrimidine (4), 2-amino-5-nitroso-4,6-bis(3-pyridylmethoxy)pyrimidine (5) and 2-amino-4,6-bis(2-hydroxyethylamino)-5-nitrosopyrimidine (6). Compounds (2)–(6) prove to exhibit highly polarized molecular–electronic structures, and in all of the compounds studied here, the supramolecular aggregation is dominated by hard hydrogen bonds, principally of N—H···N and N—H···O types.

© 2004 International Union of Crystallography
Printed in Great Britain – all rights reserved

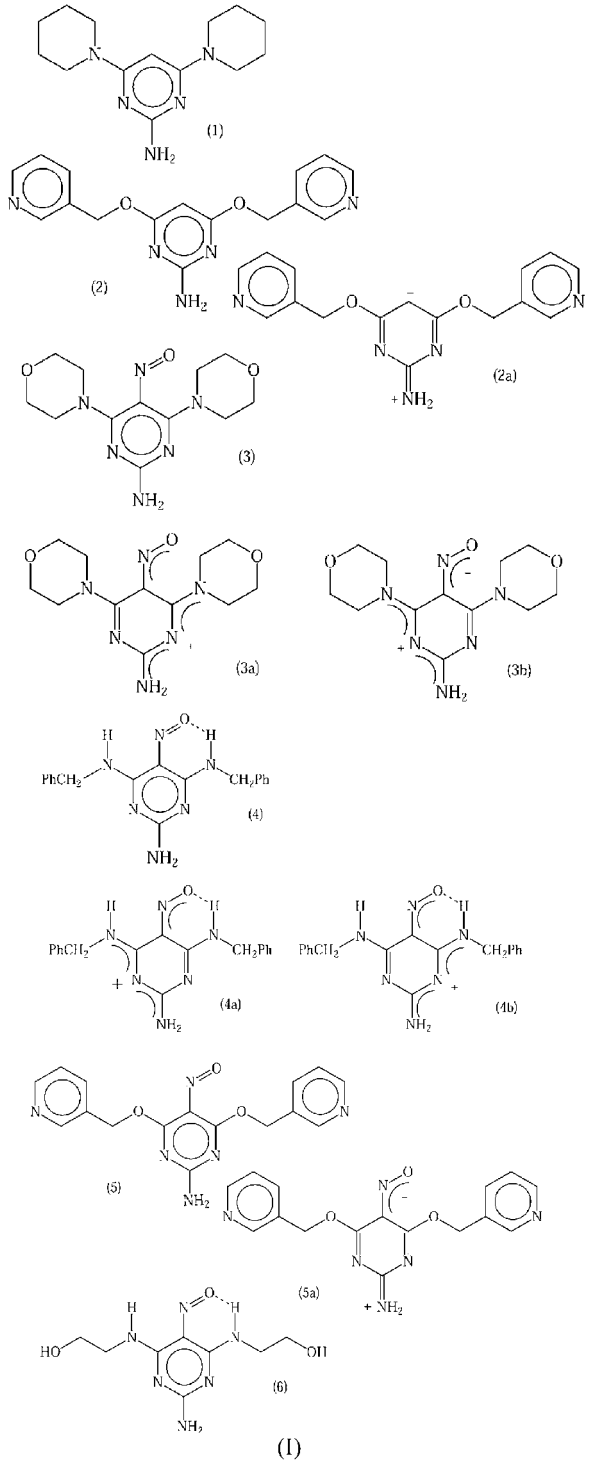

2. Experimental

2.1. Synthesis

Compound (1) was prepared by the reaction of 2-amino-4,6-dichloropyrimidine (purchased from Aldrich) with 2.5 molar equivalents of piperidine in refluxing 2-propanol. Compound (2) was similarly prepared from 2-amino-4,6-dichloropyrimidine and sodium 3-pyridylmethoxide, and then converted to (5) using the nitrosation methodology of Marchal *et al.* (2002). Compounds (3), (4) and (6) were prepared by the treatment of 2-amino-4,6-dimethoxy-5-nitrosopyrimidine (Glidewell *et al.*, 2002) with 2 molar equivalents of morpholine, benzylamine or 2-ethanolamine, respectively, all in aqueous solution at room temperature.

Crystals suitable for single-crystal X-ray diffraction were obtained by slow evaporation of solutions in the solvents specified: (1), ethyl acetate (colourless prisms, m.p. 458 K); (2), hexane–diethyl ether (1/1, v/v; colourless plates, m.p. 404 K); (3), acetonitrile–dimethylsulfoxide (5/1, v/v; red blocks, m. p. 463 K); (4), acetonitrile–ethanol–water (1/1/1 by volume; violet plates, m.p. 443 K); (5), acetonitrile–ethanol–water (1/1/1 by volume; blue blocks, m.p. 456 K); (6), acetone–methanol (1/1, v/v; red blocks, m.p. 488 K).

2.2. Data collection, structure solution and refinement

Diffraction data were collected at 120 (2) K using a Nonius Kappa-CCD diffractometer with graphite-monochromated Mo $K\alpha$ radiation (λ = 0.71073 Å). Other details of cell data, data collection and refinement are summarized in Table 1, together with details of the software employed (Ferguson, 1999; Nonius, 1997; Otwinowski & Minor, 1997; Sheldrick, 1997*a*,*b*; Spek, 2003).

For each of compounds (1), (3), (4) and (6) the space group $P2_1/c$ was uniquely assigned from the systematic absences, while the space group $P2_12_12_1$ was similarly assigned for (5). Compound (2) is triclinic and the space group $P\bar{1}$ was selected and confirmed by the subsequent structure analysis; although $Z' = 3$ for (2), ADDSYM (Spek, 2003) revealed no additional symmetry. The structures were solved by direct methods and refined with all data on F^2. A weighting scheme based upon $P = [F_o^2 + 2F_c^2]/3$ was employed in order to reduce the statistical bias (Wilson, 1976). All H atoms were located from difference maps and included in the refinements as riding atoms with distances O—H 0.84, N—H 0.88 and C—H 0.95 (aromatic) or 0.99 Å (CH_2). In the absence of any significant anomalous scattering for (5), the Flack parameter (Flack, 1983) was indeterminate (Flack & Bernardinelli, 2000) and thus the correct orientation of the structure with respect to the polar axes could not be determined. Accordingly, the Friedel equivalents were merged prior to the final refinement. It became apparent at an early stage in the refinement for (6) that both of the 2-hydroxyethyl substituents, and the nitroso substituent, were all disordered: each substituent was modelled using two sets of sites, with the occupancies for the 2-hydroxyethyl substituents given common values which refined to 0.819 (3) and 0.191 (3): the occupancies of the nitroso fragments refined to 0.68 (2) and 0.32 (2), and they were fixed at these values in the final refinements.

Supramolecular analyses were made, and the diagrams were prepared, with the aid of *PLATON* (Spek, 2003). Details of the pyrimidine ring-puckering are given in Table 2, and hydrogen-bond dimensions are given in Table 3.[1] Figs. 1–19

[1] Supplementary data for this paper are available from the IUCr electronic archives (Reference: NA5007). Services for accessing these data are described at the back of the journal.

Table 1
Experimental details.

	I	II	III
Crystal data			
Chemical formula	$C_{14}H_{23}N_5$	$C_{16}H_{15}N_5O_2$	$C_{12}H_{18}N_6O_3$
M_r	261.37	309.33	294.32
Cell setting, space group	Monoclinic, $P2_1/c$	Triclinic, $P\bar{1}$	Monoclinic, $P2_1/c$
a, b, c (Å)	12.1473 (4), 9.8811 (3), 11.4068 (3)	11.3545 (3), 12.7528 (4), 16.9511 (6)	13.0037 (4), 9.1130 (3), 12.4892 (3)
α, β, γ (°)	90.00, 96.6490 (1), 90.00	70.038 (1), 73.206 (1), 79.626 (1)	90.00, 112.3400 (12), 90.00
V (Å^3)	1359.93 (7)	2199.62 (12)	1368.92 (7)
Z	4	6	4
D_x (Mg m^{-3})	1.277	1.401	1.428
Radiation type	Mo $K\alpha$	Mo $K\alpha$	Mo $K\alpha$
No. of reflections for cell parameters	3100	9847	3096
θ range (°)	3.1–27.5	2.9–27.5	3.0–27.5
μ (mm^{-1})	0.08	0.10	0.11
Temperature (K)	120 (2)	120 (2)	120 (2)
Crystal form, colour	Block, orange	Plate, colourless	Block, blue
Crystal size (mm)	0.35 × 0.30 × 0.22	0.40 × 0.20 × 0.05	0.30 × 0.20 × 0.20
Data collection			
Diffractometer	Kappa-CCD	Kappa-CCD	Kappa-CCD
Data collection method	ϕ scans, and ω scans with κ offsets	ϕ scans, and ω scans with κ offsets	ϕ scans, and ω scans with κ offsets
Absorption correction	Multi-scan	None	None
T_{min}	0.968	–	–
T_{max}	0.983	–	–
No. of measured, independent and observed reflections	13 657, 3100, 2195	32 137, 9847, 4349	10 906, 3096, 2391
Criterion for observed reflections	$I > 2\sigma(I)$	$I > 2\sigma(I)$	$I > 2\sigma(I)$
R_{int}	0.069	0.086	0.047
θ_{max} (°)	27.5	27.5	27.5
Range of h, k, l	$-15 \Rightarrow h \Rightarrow 15$ $-10 \Rightarrow k \Rightarrow 12$ $-14 \Rightarrow l \Rightarrow 14$	$-14 \Rightarrow h \Rightarrow 14$ $-16 \Rightarrow k \Rightarrow 16$ $-22 \Rightarrow l \Rightarrow 22$	$-16 \Rightarrow h \Rightarrow 16$ $-11 \Rightarrow k \Rightarrow 10$ $-14 \Rightarrow l \Rightarrow 16$
Refinement			
Refinement on	F^2	F^2	F^2
$R[F^2 > 2\sigma(F^2)]$, $wR(F^2)$, S	0.049, 0.128, 1.02	0.058, 0.148, 0.90	0.043, 0.114, 1.04
No. of reflections	3100	9847	3096
No. of parameters	172	622	190
H-atom treatment	Constrained to parent site	Constrained to parent site	Constrained to parent site
Weighting scheme	$w = 1/[\sigma^2(F_o^2) + (0.066P)^2 + 0.176P]$, where $P = (F_o^2 + 2F_c^2)/3$	$w = 1/[\sigma^2(F_o^2) + (0.0648P)^2]$, where $P = (F_o^2 + 2F_c^2)/3$	$w = 1/[\sigma^2(F_o^2) + (0.0615P)^2 + 0.2156P]$, where $P = (F_o^2 + 2F_c^2)/3$
$(\Delta/\sigma)_{max}$	<0.0001	<0.0001	0.001
$\Delta\rho_{max}$, $\Delta\rho_{min}$ (e Å^{-3})	0.20, −0.29	0.30, −0.34	0.41, −0.28

	IV	V	VI
Crystal data			
Chemical formula	$C_{18}H_{18}N_6O$	$C_{16}H_{14}N_6O_3$	$C_8H_{14}N_6O_3$
M_r	334.38	338.33	242.25
Cell setting, space group	Monoclinic, $P2_1/c$	Orthorhombic, $P2_12_12_1$	Monoclinic, $P2_1/c$
a, b, c (Å)	12.9416 (1), 6.6816 (3), 20.0033 (5)	6.881 (2), 9.140 (3), 24.4636 (10)	9.6487 (1), 14.8594 (2), 7.3497 (2)
β (°)	113.3020 (12)	90.00	101.097 (1)
V (Å^3)	1588.61 (8)	1538.6 (7)	1034.05 (3)
Z	4	4	4
D_x (Mg m^{-3})	1.398	1.461	1.556
Radiation type	Mo $K\alpha$	Mo $K\alpha$	Mo $K\alpha$
No. of reflections for cell parameters	3618	2026	2366
θ range (°)	3.3–27.5	3.3–27.5	3.1–27.5
μ (mm^{-1})	0.09	0.11	0.12
Temperature (K)	120 (2)	120 (2)	120 (2)
Crystal form, colour	Plate, purple	Plate, colourless	Rod, orange
Crystal size (mm)	0.42 × 0.12 × 0.03	0.45 × 0.12 × 0.04	0.20 × 0.06 × 0.04
Data collection			
Diffractometer	Kappa-CCD	Kappa-CCD	Kappa-CCD
Data collection method	ϕ scans, and ω scans with κ offsets	ϕ scans, and ω scans with κ offsets	ϕ scans, and ω scans with κ offsets
Absorption correction	Multi-scan	None	None
T_{min}	0.957	–	–
T_{max}	0.997	–	–
No. of measured, independent and observed reflections	27 586, 3618, 2492	8813, 2026, 1369	14 888, 2366, 1928

Table 1 (continued)

	IV	V	VI
Criterion for observed reflections	$I > 2\sigma(I)$	$I > 2\sigma(I)$	$I > 2\sigma(I)$
R_{int}	0.099	0.067	0.039
θ_{max} (°)	27.5	27.5	27.5
Range of h, k, l	$-16 \Rightarrow h \Rightarrow 16$ $-8 \Rightarrow k \Rightarrow 8$ $-25 \Rightarrow l \Rightarrow 25$	$-7 \Rightarrow h \Rightarrow 8$ $-11 \Rightarrow k \Rightarrow 8$ $-29 \Rightarrow l \Rightarrow 31$	$-12 \Rightarrow h \Rightarrow 12$ $-19 \Rightarrow k \Rightarrow 19$ $-9 \Rightarrow l \Rightarrow 8$
Refinement			
Refinement on	F^2	F^2	F^2
$R[F^2 > 2\sigma(F^2)]$, $wR(F^2)$, S	0.046, 0.120, 1.01	0.049, 0.100, 1.00	0.066, 0.180, 1.04
No. of reflections	3618	2026	2366
No. of parameters	226	226	180
H-atom treatment	Constrained to parent site	Constrained to parent site	Constrained to parent site
Weighting scheme	$w = 1/[\sigma^2(F_o^2) + (0.0597P)^2 + 0.3316P]$, where $P = (F_o^2 + 2F_c^2)/3$	$w = 1/[\sigma^2(F_o^2) + (0.0483P)^2]$, where $P = (F_o^2 + 2F_c^2)/3$	$w = 1/[\sigma^2(F_o^2) + (0.0886P)^2 + 1.0053P]$, where $P = (F_o^2 + 2F_c^2)/3$
$(\Delta/\sigma)_{max}$	<0.0001	<0.0001	0.001
$\Delta\rho_{max}$, $\Delta\rho_{min}$ (e Å^{-3})	0.27, −0.34	0.21, −0.28	0.55, −0.37

Computer programs used: *Kappa-CCD* (Nonius, 1997), *DENZO-SMN* (Otwinowski & Minor, 1997), *SHELXS*97 (Sheldrick, 1997*b*), *SHELXL*97 (Sheldrick, 1997*a*), *PLATON* (Spek, 2003), *PRPKAPPA* (Ferguson, 1999).

show the molecular components with the atom-labelling schemes and aspects of the supramolecular structures.

3. Results and discussion

3.1. Molecular conformations

In (2) and (5) the 3-pyridylmethoxy substituents all adopt conformations with the atoms C*mn*7 and C*mn*1 [m = 1, 2 or 3 for (2), 0 for (5); n = 4 or 6] essentially in the plane of the pyrimidine ring with fully extended chain fragments C*mn*—O*mn*—C*mn*7—C*mn*1 (Figs. 4 and 12). In this respect, (2) and (5) resemble (7) (Quesada, Low *et al.*, 2002) and (8) (Quesada, Marchal *et al.*, 2002) [see Scheme (II)]. However, the conformations adopted by the pyridyl rings relative to the remainder of the molecules differ not only between (2) and (5), but also between the three independent molecules in (2): this, together with the hydrogen-bonding patterns adopted by these molecules (see §3.3 below), precludes the possibility of any additional symmetry in (2).

In contrast with (2) and (5), in (4) both benzylamino substituents adopt conformations in which the torsional angles C*n*—N*n*—C*n*7—C*n*1 (n = 4 or 6) are approximately −90°, so that the atoms C41 and C61 are well removed from the plane of the pyrimidine ring. Hence, with the exception of the nitroso group, the remaining atoms in the molecule of (4) adopt a conformation which is close to having twofold rotational symmetry (Fig. 10). In (6), on the other hand, the major orientations of the two independent 2-hydroxyethylamino substituents adopt entirely different conformations, as do the minor orientations also. In this compound only, the nitroso group is disordered over two orientations, with the O atoms directed towards the N4—H4 bond in the major form and towards the N6—H6 bond in the minor form.

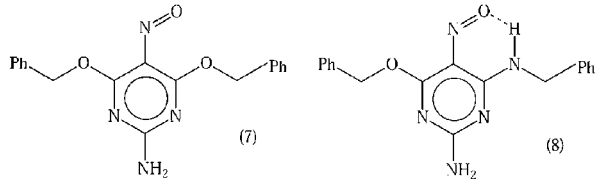

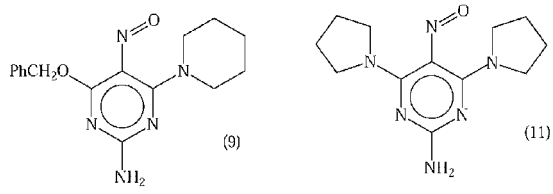

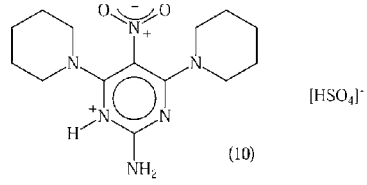

(II)

In (1) and (3) the piperidine and morpholine rings adopt chair conformations, as expected (Figs. 1 and 7): in both compounds the N4 and N6 atoms each have essentially coplanar bonds and the orientations of these rings around the C4—N4 and C6—N6 bonds are such as to maximize the overlap of the lone-pair orbitals at N4 and N6 with the π-orbitals of the pyrimidine rings.

Perhaps the most striking aspect of the conformations adopted by these molecules is the markedly non-planar pyrimidine ring conformation in (3). The six torsional angles within this ring, although not independent as they must sum to

Table 2
Selected intramolecular distances and bond orders.

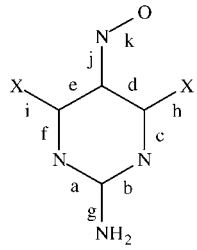

a	*b*	*c*	*d*	*e*	*f*	*g*	*h*	*i*	*j*	*k*	Δ
(*a*) Bond distances (Å)											
(1)											
1.341 (2)	1.344 (2)	1.349 (2)	1.400 (2)	1.395 (2)	1.356 (2)	1.355 (2)	1.373 (2)	1.379 (2)	–	–	–
(2)											
1.354 (3)	1.353 (3)	1.318 (3)	1.391 (3)	1.378 (3)	1.318 (3)	1.332 (3)	1.359 (3)	1.366 (3)	–	–	–
1.357 (3)	1.365 (3)	1.319 (3)	1.390 (3)	1.391 (3)	1.320 (3)	1.327 (3)	1.363 (3)	1.357 (3)	–	–	–
1.361 (3)	1.352 (3)	1.324 (3)	1.391 (3)	1.383 (3)	1.322 (3)	1.331 (3)	1.360 (3)	1.362 (3)	–	–	–
(3)											
1.344 (2)	1.357 (2)	1.335 (2)	1.455 (2)	1.452 (2)	1.337 (2)	1.329 (2)	1.342 (2)	1.341 (2)	1.362 (2)	1.267 (2)	0.095
(4)											
1.357 (2)	1.359 (2)	1.341 (2)	1.450 (2)	1.450 (2)	1.339 (2)	1.332 (2)	1.332 (2)	1.332 (2)	1.342 (2)	1.287 (2)	0.055
(5)											
1.367 (4)	1.363 (4)	1.307 (4)	1.420 (4)	1.438 (4)	1.312 (4)	1.307 (4)	1.346 (3)	1.325 (4)	1.372 (4)	1.252 (4)	0.120
(6)†											
1.359 (3)	1.356 (3)	1.337 (3)	1.448 (3)	1.450 (3)	1.331 (3)	1.331 (3)	1.323 (3)	1.330 (3)	1.346 (4)	1.284 (4)	0.062
(*b*) Bond orders											
(1)											
1.65	1.64	1.61	1.64	1.67	1.57	1.58	1.48	1.45	–	–	
(2)											
1.58	1.59	1.79	1.69	1.76	1.79	1.71	1.26	1.23	–	–	
1.56	1.52	1.78	1.70	1.69	1.78	1.74	1.24	1.27	–	–	
1.54	1.59	1.75	1.69	1.74	1.77	1.71	1.26	1.25	–	–	
(3)											
1.64	1.56	1.69	1.36	1.38	1.68	1.72	1.65	1.65	1.54	1.72	
(4)											
1.56	1.55	1.65	1.39	1.39	1.67	1.71	1.71	1.71	1.65	1.63	
(5)											
1.51	1.53	1.86	1.54	1.45	1.83	1.86	1.32	1.41	1.48	1.79	
(6)†											
1.55	1.57	1.68	1.40	1.39	1.71	1.71	1.76	1.72	1.63	1.65	

$\Delta = j - k$. † Major orientations only.

zero, show a striking pattern in that corresponding pairs have similar magnitudes with opposite signs, indicative of approximate mirror symmetry across the plane defined by atoms N2, C2, C5 and N5. To investigate this further, we can define the plane through the atoms C2, C4 and C6 as a reference plane and then consider the displacements of the other ring atoms, and the exocyclic atoms, from this plane. The displacements of the other ring atoms are N1 −0.063 (2), N3 −0.090 (2) and C5 +0.284 (2) Å (the absolute signs are arbitrary, but opposite signs indicate displacements to opposite sides of the reference plane): for the immediate exocyclic atoms the corresponding displacements are N2 +0.095 (3), N4 −0.111 (2) Å, N5 +1.155 (2) and N6 −0.156 (3) Å. These displacements are clearly indicative of a boat or sofa conformation for the pyrimidine ring in (3) having a local pseudo-mirror plane containing the atoms N2, C2, C5 and N5 (Fig. 8), and the ring-

puckering parameters (Cremer & Pople, 1975; Cremer, 1984; Evans & Boeyens, 1989) corresponding to the atom-sequence N1–C6, Q = 0.207 (2) Å, φ = 63.9 (4)°, θ = 104.9 (4)°, are entirely consistent with this (Boeyens, 1978). This pyrimidine ring conformation may be contrasted with the twist-boat conformations observed in each of compounds (9) (Melguizo *et al.*, 2003), (10) (Quesada *et al.*, 2003) and (11) (Quesada, Marchal *et al.*, 2002) [see Scheme (II)].

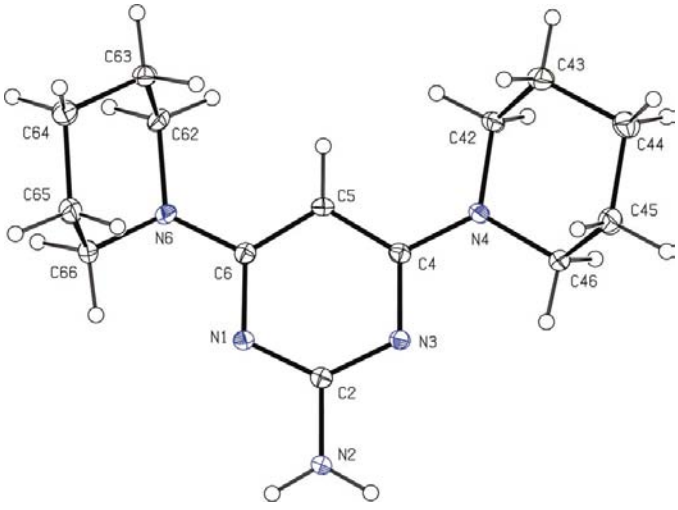

Figure 1
A molecule of (1) showing the atom-labelling scheme. Displacement ellipsoids are drawn at the 30% probability level.

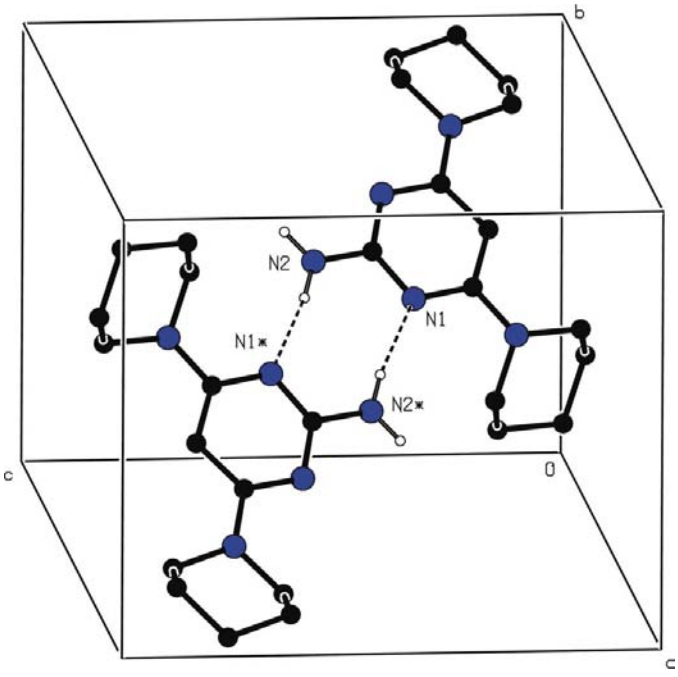

Figure 2
Part of the crystal structure of (1) showing the formation of a centrosymmetric $R_2^2(8)$ dimer. For the sake of clarity, the H atoms bonded to C atoms are omitted. The atoms marked with an asterisk (*) are at the symmetry position $(1-x, 1-y, 1-z)$.

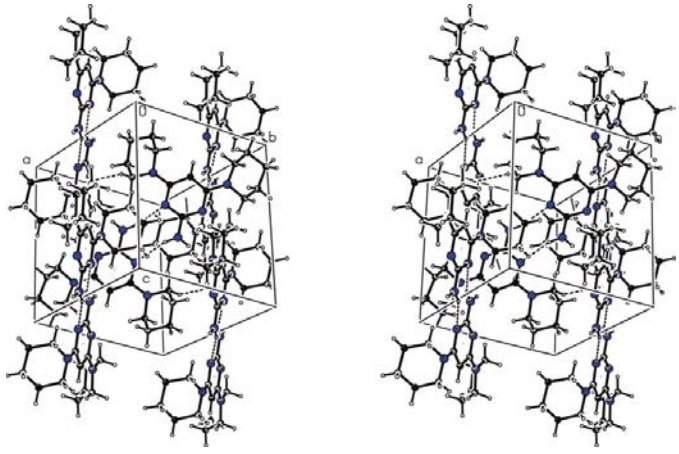

Figure 3
Stereoview of part of the crystal structure of (1) showing the linking of the $R_2^2(8)$ dimers into a (100) sheet by means of a single C—H···π(arene) hydrogen bond.

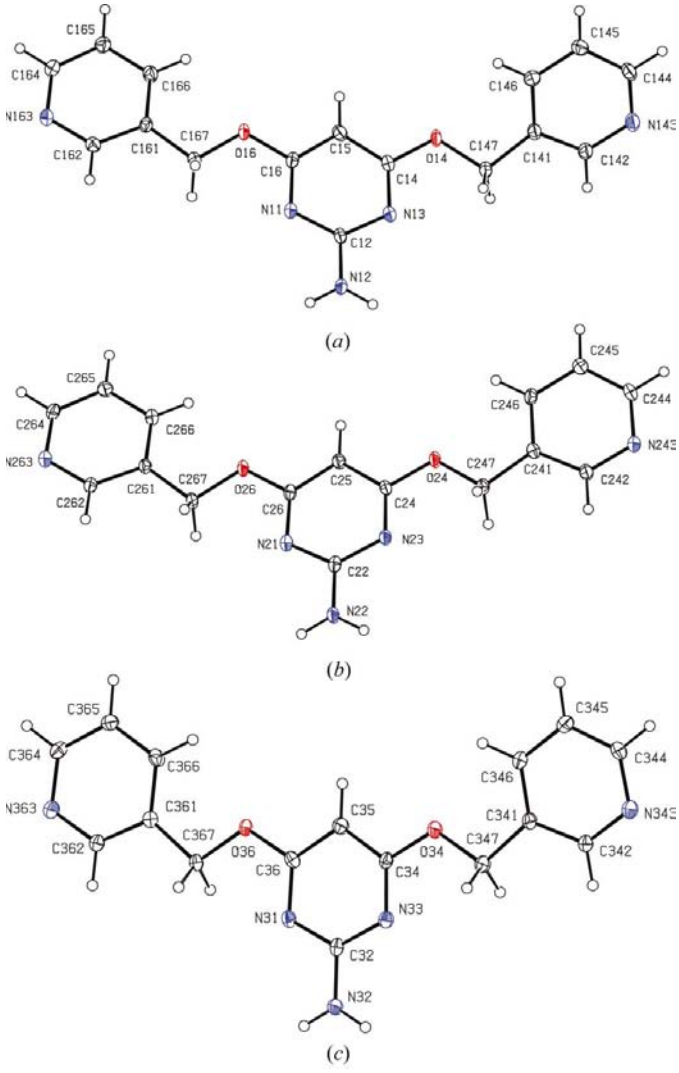

Figure 4
The three independent molecules of (2) showing the atom-labelling scheme. Displacement ellipsoids are drawn at the 30% probability level.

Table 3
Hydrogen-bond parameters (Å, °).

D—H···A	H···A	D···A	D—H···A
(1)			
N2—H2A···N1^{i}	2.37	3.216 (2)	162
C66—H66B···Cg1^{ii}†	2.68	3.518 (2)	142
(2)			
N12—H12A···N363	2.12	2.998 (3)	174
N12—H12B···N343^{iii}	2.10	2.977 (3)	176
N22—H22A···N263^{iv}	2.11	2.985 (3)	175
N22—H22B···N243^{v}	2.11	2.987 (3)	175
N32—H32A···N143	2.11	2.978 (3)	167
N32—H32B···N163^{vi}	2.10	2.982 (3)	178
(3)			
N2—H2A···O64^{ii}	2.04	2.918 (2)	177
N2—H2B···O44^{vii}	2.13	2.894 (2)	144
C43—H43A···O5^{vii}	2.47	3.376 (2)	152
(4)			
N2—H2A···N3^{ii}	2.19	3.042 (2)	163
N2—H2B···N1^{viii}	2.15	2.967 (2)	155
N4—H4···O5^{ix}	2.15	2.993 (2)	161
N6—H6···O5	1.94	2.617 (2)	133
C63—H63···O5^{x}	2.51	3.335 (2)	146
(5)			
N2—H2A···N43^{ii}	2.03	2.878 (4)	163
N2—H2B···N63^{xi}	2.02	2.888 (4)	171
C65—H65···Cg2^{xii}‡	2.69	3.526 (4)	148
(6)			
N2—H2A···N3^{xiii}	2.46	3.293 (3)	158
N2—H2B···O6^{xiv}	2.25	3.013 (3)	146
N4—H4···O5	1.95	2.628 (3)	133
O4—H4A···N1^{xv}	2.12	2.909 (2)	156
O6—H6A···O5^{xvi}	1.86	2.659 (4)	159

Symmetry codes: (i) $1-x, 1-y, 1-z$; (ii) $1-x, -\frac{1}{2}+y, \frac{1}{2}-z$; (iii) $1+x, 1+y, -1+z$; (iv) $1-x, 2-y, -z$; (v) $-x, 1-y, 1-z$; (vi) $-1+x, -1+y, 1+z$; (vii) $-x, -\frac{1}{2}+y, -\frac{1}{2}-z$; (viii) $1-x, \frac{1}{2}+y, \frac{1}{2}-z$; (ix) $-x, \frac{1}{2}+y, \frac{1}{2}-z$; (x) $-x, 1-y, -z$; (xi) $-\frac{1}{2}+x, \frac{3}{2}-y, -z$; (xii) $-\frac{1}{2}+x, \frac{5}{2}-y, -z$; (xiii) $1-x, -y, -z$; (xiv) $x, \frac{1}{2}-y, \frac{1}{2}+z$; (xv) $1+x, y, z$; (xvi) $1-x, 1-y, -z$. † Cg1 is the centroid of the ring N1–C6. ‡ Cg2 is the centroid of the ring N63, C61–C66.

Pyrimidine ring puckering of this type may most plausibly be considered as resulting from the presence of three adjacent substituents as positions 4, 5 and 6 of the pyrimidine ring, two of them sterically demanding, and with no possibility of intramolecular hydrogen bonding between them, all of which are attempting to maximize the extent of conjugative overlap with the pyrimidine ring. When the substituents at positions 4 and 6 are alkoxyl, as in (5) or primary amino, as in (4) and (6), there is no steric clashing to drive the pyrimidine ring-puckering. However, when the substituents at positions 4 and 6 are secondary amino, as in (3), maximum orbital overlap is incompatible with the maintenance of a planar pyrimidine ring. Rather than the substituents rotating about the exocyclic C—N bonds to avoid steric clashing, instead the ring puckers with adjacent substituents displaced towards opposite faces of the ring.

In summary, significant puckering of the pyrimidine ring occurs when secondary amino substituents flank either a nitroso or a nitro group.

3.2. Molecular dimensions

The intramolecular bond distances in (1)–(6) (Table 2) show a number of unusual values, as compared with typical values (Allen *et al.*, 1987) for bonds of similar types, and these point in many cases to significantly polarized molecular–electronic structures, particularly in those compounds containing nitroso substituents.

Compound (1), where there is no nitroso group and three simple amino substituents, serves as a benchmark for this series: in this compound, the pyrimidine ring C—N distances *a*, *b*, *c* and *f* (Table 2) span a rather small range, while the exocyclic C—N distances *g*, *h* and *i* are typical of those for bonds of types C(ar)—NH_2 and C(ar)—NR_2 (the mean values are 1.355 and 1.371 Å, respectively, for bonds involving planar N in each case). The molecular–electronic structure of (1) is therefore best represented as the classically delocalized aromatic form [see Scheme (I)]. The three independent molecules in (2) all exhibit very similar distances, but there is

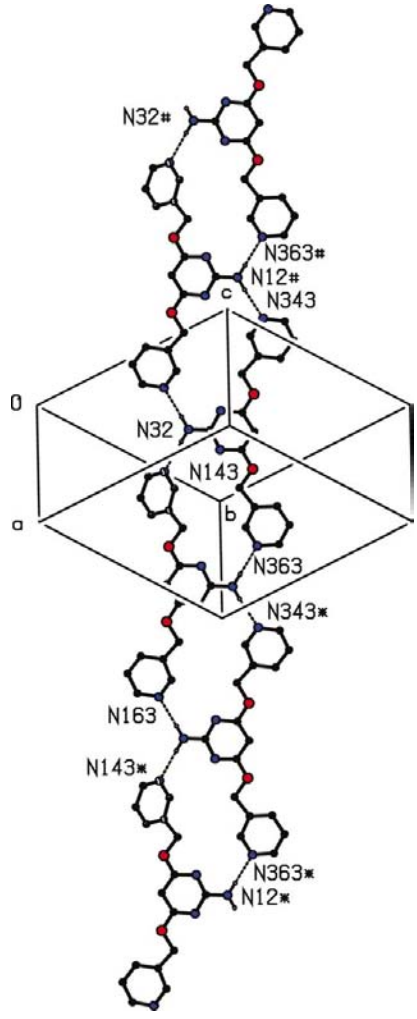

Figure 5
Part of the crystal structure of (2) showing the formation of the [11$\bar{1}$] chain generated by translation. For the sake of clarity the H atoms bonded to C atoms are omitted. The atoms marked with an asterisk (*) or a hash (#) are at the symmetry positions $(1+x, 1+y, -1+z)$ and $(-1+x, -1+y, 1+z)$, respectively.

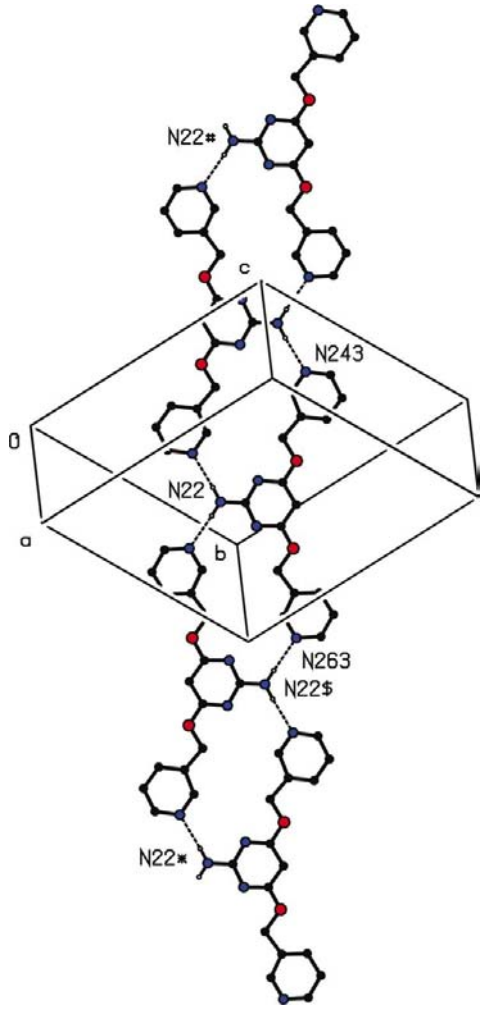

Figure 6
Part of the crystal structure of (2) showing the formation of the [11$\bar{1}$] chain generated by inversion. For the sake of clarity the H atoms bonded to C atoms are omitted. The atoms marked with an asterisk (*), a hash (#) or a dollar sign ($) are at the symmetry positions $(1+x, 1+y, -1+z)$, $(-1+x, -1+y, 1+z)$ and $(1-x, 2-y, -z)$, respectively.

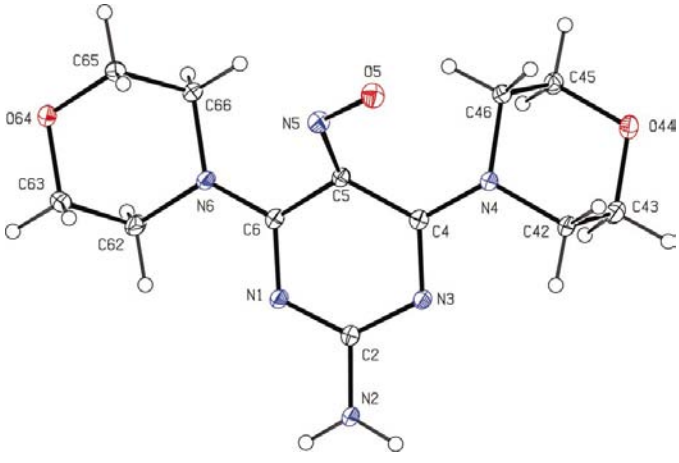

Figure 7
A molecule of (3) showing the atom-labelling scheme. Displacement ellipsoids are drawn at the 30% probability level.

now a clear distinction between the longer pyrimidine ring C—N bonds *a* and *b* on the one hand, and the shorter bonds *c* and *f* on the other: in addition, the exocyclic bond *g* is significantly shorter in (2) than it is in (1). These observations suggest that the polarized form (2*a*) is an additional contributor to the overall molecular–electronic structure, alongside the aromatic form (2).

In (3) all of the pyrimidine ring distances *a*, *b*, *c* and *f*, and the exocyclic C—N bonds *g*, *h* and *i* lie in the comparatively narrow range 1.329 (2)–1.357 (2) Å; at the same time, the pyrimidine C—C distances *d* and *e* are both long, compared with the corresponding bonds in (1) and (2). In addition, the difference Δ between the nitroso bonds *j* and *k* is only 0.095 Å, as compared with a difference in excess of 0.20 Å generally found in simple C-nitroso compounds where there is no possibility of significant electronic delocalization (Talberg, 1977; Schlemper *et al.*, 1986). These observations, taken all together, point to the two forms (3*a*) and (3*b*) as the dominant contributors to the overall molecular–electronic structure. It should be emphasized here that extensive polarization is clearly possible, despite the marked puckering of the pyrimidine ring into a boat conformation (see §3.1, above). Similar polarization to that in (3) also occurs in (4), where the pyrimidine ring is planar, but it appears to be more pronounced with an even smaller value of Δ, forming (4*a*) and (4*b*). Insofar as the extensive disorder in (6) permits detailed consideration of the intramolecular dimensions, the behaviour of this compound appears to be very similar to that of (4). Yet a different form of electronic polarization is evident in (5), where the ring C—N bonds *c* and *f* are much shorter than bonds *a* and *b*, and the exocyclic C—N bond *g* is likewise very

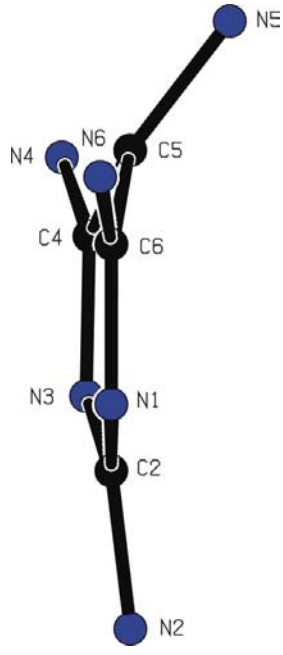

Figure 8
Part of a molecule of (3) showing the markedly non-planar conformation of the pyrimidine ring.

short for its type, indicating form (5*a*) as the dominant contributor.

An alternative way to visualize the consequences of the molecular–electronic structure is by means of the corresponding bond orders (Table 2), calculated using the recent recalibration by Kotelevskii & Prezhdo (2001) of the original equation relating bond order to bond length (Gordy, 1947). Comparison of the values for the pyrimidine ring bonds *a*–*f* in (1) and (2) emphasizes the polarization in (2), while each of the nitrosated compounds (3)–(6) exhibits rather similar values for the bonds *j* and *k*. The bond orders also point up the bond fixation in (5), with very high values for bonds *c*, *f* and *g*.

3.3. Supramolecular structures

The extensively polarized molecular–electronic structures lead to the development of charge-assisted hydrogen bonding (Gilli *et al.*, 1994).

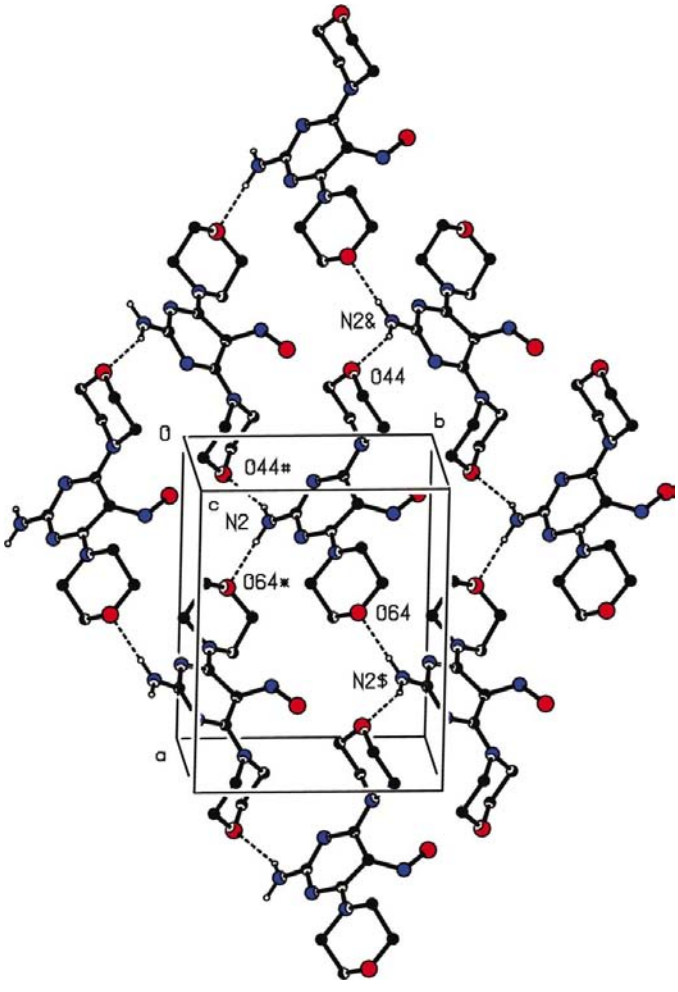

Figure 9
Part of the crystal structure of (3) showing the formation of a $(10\bar{1})$ sheet of $R_4^4(32)$ rings. For the sake of clarity, the H atoms bonded to C atoms are omitted. The atoms marked with an asterisk (*), a hash (#), a dollar sign ($) or an ampersand (&) are at the symmetry positions $(1-x, -\frac{1}{2}+y, \frac{1}{2}-z)$, $(-x, -\frac{1}{2}+y, -\frac{1}{2}-z)$, $(1-x, \frac{1}{2}+y, \frac{1}{2}-z)$ and $(-x, \frac{1}{2}+y, -\frac{1}{2}-z)$, respectively.

3.3.1. Hard hydrogen bonds generate a finite, zero-dimensional structure. The supramolecular aggregation of (1) takes the form of a centrosymmetric dimer formed by paired N—H···N hydrogen bonds forming an $R_2^2(8)$ motif (Fig. 2). Dimers of this kind are linked by a single C—H···π(arene) hydrogen bond. Atoms of the type C66 in the molecules at (x, y, z) and $(1-x, 1-y, 1-z)$, which comprise the dimer centred at (0.5, 0.5, 0.5), act respectively as hydrogen-bond donors, *via* H66*B*, to the pyrimidine rings of the molecules at $(1-x, -\frac{1}{2}+y, \frac{1}{2}-z)$ and $(x, \frac{3}{2}-y, \frac{1}{2}+z)$, which form parts of the $R_2^2(8)$ dimers centred at (0.5, 0, 0) and (0.5, 1, 1). In like manner the pyrimidine rings at (x, y, z) and $(1-x, 1-y, 1-z)$ accept hydrogen bonds from atoms C66 in the molecules at $(1-x, \frac{1}{2}+y, \frac{1}{2}-z)$ and $(x, \frac{1}{2}-y, \frac{1}{2}+z)$, which lie respectively in the dimers centred at (0.5, 1, 0) and

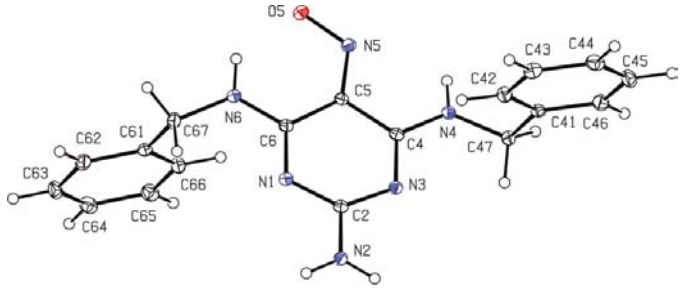

Figure 10
The molecule of (4) showing the atom-labelling scheme. Displacement ellipsoids are drawn at the 30% probability level.

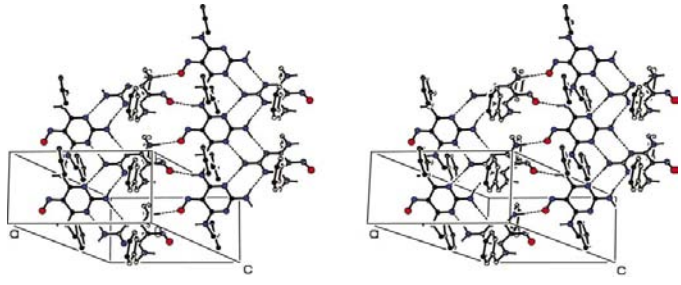

Figure 11
Stereoview of part of the crystal structure of (4) showing the formation of a (001) sheet by the linking of [010] chains of rings. For the sake of clarity the H atoms bonded to C atoms are omitted.

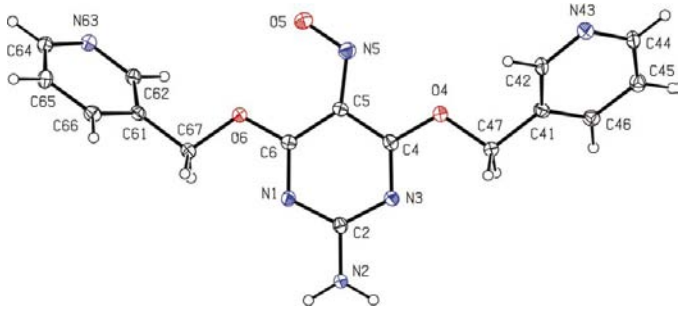

Figure 12
A molecule of (5) showing the atom-labelling scheme. Displacement ellipsoids are drawn at the 30% probability level.

(0.5, 0, 1). In this manner, the single soft (Desiraju & Steiner, 1999) hydrogen bond links the $R_2^2(8)$ dimers into a (100) sheet (Fig. 3). It is noteworthy in this connection that the N2—H2*B* bond plays no part in the supramolecular aggregation, forming neither an N—H···N nor an N—H···π(arene) hydrogen bond.

3.3.2. Hard hydrogen bonds generate a one-dimensional structure. Compound (2) crystallizes in the space group $P\bar{1}$ with $Z' = 3$ (Fig. 4). Despite this, the supramolecular structure is remarkably simple, although rather unusual. Each amino group acts as a double donor in N—H···N hydrogen bonds, and in each molecule the two N atoms in the 3-pyridylmethanol substituents act as the acceptors. One of the molecules, arbitrarily labelled here as molecule 2 containing N22 *etc.*, forms a chain of edge-fused $R_2^2(20)$ rings generated by inversion, while the other two molecules together form a similar chain generated by translation.

The amino N12 atom in the molecule of type 1 at (x, y, z) acts as a hydrogen-bond donor, *via* H12*A* and H12*B*, respectively, to the pyridyl N363 atom at (x, y, z) and N343 atom at $(1 + x, 1 + y, -1 + z)$. Similarly, the amino N32 atom in the type 3 molecule at (x, y, z) acts as a donor, *via* H32*A* and H32*B*, respectively, to the pyridyl N143 atom at (x, y, z) and N163 atom at $(-1 + x, -1 + y, 1 + z)$. The combined effect of these four N—H···N hydrogen bonds is to generate by translation a chain of edge-fused rings, containing two distinct $R_2^2(20)$ rings, running parallel to the $[11\bar{1}]$ direction (Fig. 5). In molecule 2, the amino N22 atom at (x, y, z) acts as a hydrogen-bond donor, *via* H22*A* and H22*B*, respectively, to the pyridyl N263 atom at $(1 - x, 2 - y, -z)$ and N243 atom at $(-x, 1 - y, 1 - z)$, thereby generating two centrosymmetric

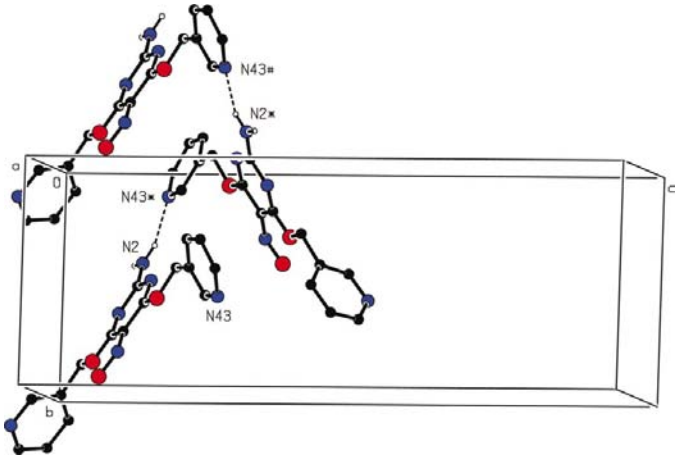

Figure 13
Part of the crystal structure of (5) showing the formation of a $C(10)$ chain along [010]. For the sake of clarity the H atoms bonded to C atoms are omitted. The atoms marked with an asterisk (*) or a hash (#) are at the symmetry positions $(1 - x, -\frac{1}{2} + y, \frac{1}{2} - z)$ and $(x, -1 + y, z)$, respectively.

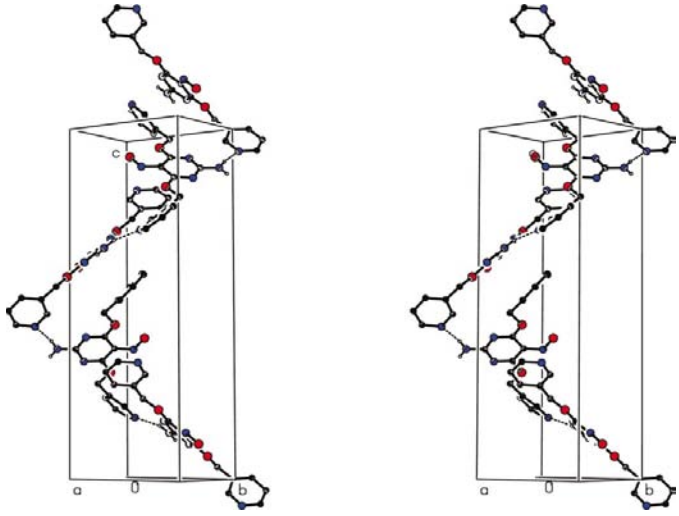

Figure 15
Stereoview of part of the crystal structure of (5) showing the formation of a $C_2^2(20)$ chain along [001]. For the sake of clarity the H atoms bonded to C atoms are omitted.

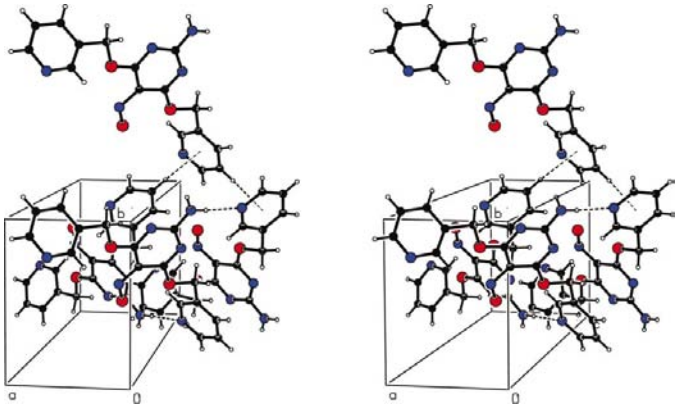

Figure 14
Stereoview of part of the crystal structure of (5) showing the formation of a $C(10)$ chain along [100] by an N—H···N hydrogen bond, and the linking of such chains into a (001) sheet by means of a C—H···π(arene) hydrogen bond.

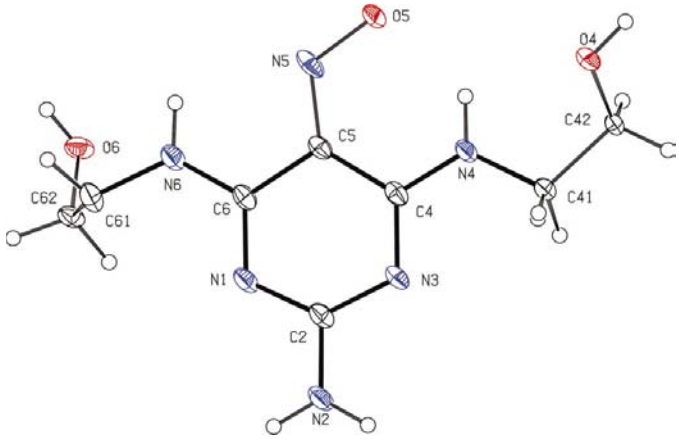

Figure 16
A molecule of (6) showing the atom-labelling scheme. Displacement ellipsoids are drawn at the 30% probability level. For the sake of clarity only the major orientation of each of the disordered fragments is shown.

$R_2^2(20)$ rings centred at (0.5, 1, 0) and (0, 0.5, 0.5). Propagation by inversion of these two hydrogen bonds thus generates a second [11$\bar{1}$] chain (Fig. 6).

A single chain of type 2 molecules passes through each unit cell, through the point (0.5, 1, 0). By contrast, two chains of type 1 and type 2 molecules, related to one another by inversion, pass through each unit cell; the mid-point of the rings containing N12 and N32 at (x, y, z) and $(1 - x, 2 - y, -z)$ lie at approximately (0.55, 0.67, 0.27) and (0.45, 1.33, −0.27), respectively. Consequently, the two chains generated by translation flank the inversion-generated chain, but there are no direction-specific interactions between adjacent chains.

It is worth noting here that despite the presence of two unencumbered pyrimidine ring N atoms in each of the three independent molecules, none of these play any role in the supramolecular aggregation. Clearly the pyridine ring N atoms are highly effective competitors here. While acid–base behaviour in aqueous solution is not necessarily a reliable guide to behaviour in the solid state, the non-participation of the pyrimidine ring N atoms in the hydrogen bonding is entirely consistent with the very much lower basicity of the ring N in simple pyrimidines (the pK_b value is typically *ca* 12.7) compared with the N in simple pyridines (pK_b typically *ca* 8.8).

3.3.3. Hard hydrogen bonds generate two-dimensional structures. In (3) (Fig. 7) the supramolecular structure is determined by just two N—H···O hydrogen bonds, with the two morpholine O atoms acting as the acceptors: there are no significant C—H···π(arene) interactions and the structure is strictly two-dimensional.

The amino N2 in the molecule at (x, y, z) acts as a hydrogen-bond donor, *via* H2*A*, to morpholine O64 in the molecule at $(1 - x, -\frac{1}{2} + y, \frac{1}{2} - z)$, thus producing a *C*(9) chain running parallel to the [010] direction and generated by the 2_1 screw axis along (0.5, *y*, 0.25). The same N2 at (x, y, z) also acts as a donor, *via* H2*B*, to morpholine O44 in the molecule at $(-x, -\frac{1}{2} + y, -\frac{1}{2} - z)$ producing a second *C*(9) chain parallel to [010], this time generated by the 2_1 axis along (0, *y*, −0.25). The combination of these two *C*(9) motifs

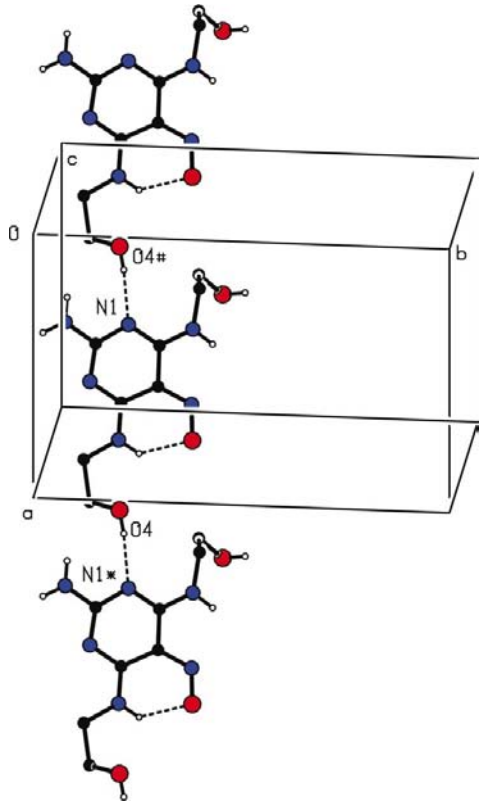

Figure 17
Part of the crystal structure of (6) showing the formation of a *C*(9) chain along [100]. The atoms marked with an asterisk (*) or a hash (#) are at the symmetry positions $(1 + x, y, z)$ and $(-1 + x, y, z)$, respectively.

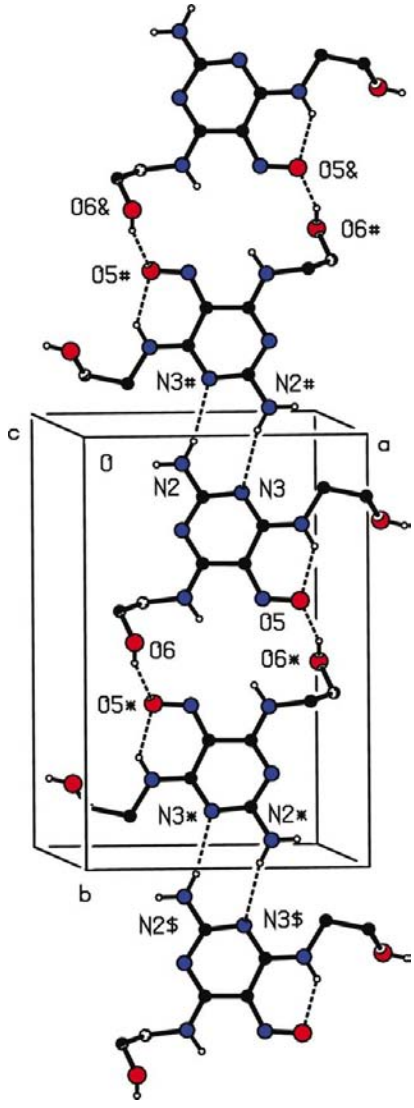

Figure 18
Part of the crystal structure of (6) showing the formation of a chain of rings along [010]. For the sake of clarity the H atoms bonded to C atoms are omitted and only the major components of the disorder are shown. The atoms marked with an asterisk (*), a hash (#), a dollar sign ($) or an ampersand (&) are at the symmetry positions $(1 - x, 1 - y, -z)$, $(1 - x, -y, -z)$, $(x, 1 + y, z)$ and $(x, -1 + y, z)$, respectively.

generates a $(10\bar{1})$ sheet in the form of a (4,4) net (Batten & Robson, 1998) built from a single type of $R_4^4(32)$ ring (Fig. 9). Two sheets of this type, related to one another by inversion, pass through each unit cell, but there are no direction-specific interactions between adjacent sheets.

There is a single C—H···O hydrogen bond in the structure, in which the morpholino atom C43 in the molecule at (x, y, z) acts as a hydrogen-bond donor to nitroso O5 in the molecule at $(-x, -\frac{1}{2}+y, -\frac{1}{2}-z)$. This interaction lies within the $(10\bar{1})$ sheet and thus does not influence the overall dimensionality of the supramolecular structure.

There are three hard (Desiraju & Steiner, 1999) hydrogen bonds in the structure of (4) (Fig. 10) and these link the molecules into (001) sheets: two of these hydrogen bonds are of the N—H···N type and the third is of the N—H···O type, and it is convenient to consider the effects of the two types in turn. The amino N2 in the molecule at (x, y, z) acts as a hydrogen-bond donor, *via* H2*A* and H2*B*, respectively, to the ring atoms N3 in the molecule at $(1-x, -\frac{1}{2}+y, \frac{1}{2}-z)$ and N1 in the molecule at $(1-x, \frac{1}{2}+y, \frac{1}{2}-z)$, thus producing a chain of edge-fused $R_2^2(8)$ rings running parallel to the [010] direction and generated by the 2_1 screw axis along (0.5, *y*, 0.25). This pattern of fused $R_2^2(8)$ rings has been observed previously (Low *et al.*, 2002; Glidewell *et al.*, 2003) in (12)–(14) [see Scheme (III)].

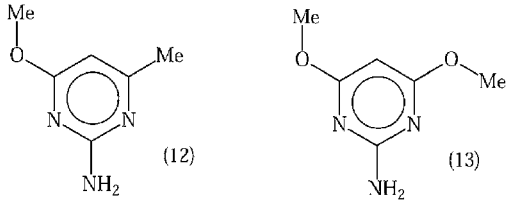

(III)

The action of the N—H···O hydrogen bond is to link adjacent chains of fused rings. Amino N4 in the molecule at (x, y, z), which lies in the (0.5, *y*, 0.25) chain acts as a hydrogen-bond donor to nitroso O5 in the molecule at $(-x, \frac{1}{2}+y, \frac{1}{2}-z)$, which is a component of the chain along (−0.5, *y*, 0.25). Propagation of this hydrogen bond thus links together into a (001) sheet (Fig. 11) all of the chains generated by screw axes having $z = 0.25$. A second sheet related to the first by inversion is generated by the screw axes at $z = 0.75$, and a single C—H···O hydrogen bonds links the adjacent sheets. The phenyl atom C63 in the molecule at (x, y, z), which is a component of the $z = 0.25$ sheet, acts as a hydrogen-bond donor to the nitroso O5 atom in the molecule at $(-x, 1-y, -z)$, which lies in the $z = -0.25$ sheet: propagation by the space group of this hydrogen bond then links together all of the (001) sheets into a single framework. Hydrogen bonds of C—H···π(arene) and N—H···π(arene) types are both absent from the structure of (4), as are aromatic $\pi\cdots\pi$ stacking interactions.

3.3.4. Hard hydrogen bonds generate three-dimensional structures. The supramolecular structure of (5) consists of a three-dimensional framework structure generated by just two N—H···N hydrogen bonds, in which the two acceptors are the pyridyl N atoms N43 and N63 (Fig. 12). It is convenient to consider the sub-structure generated by each hydrogen bond in turn and then to consider their combined effect.

The amino atom N2 in the molecule at (x, y, z) acts as a hydrogen-bond donor, *via* H2*A*, to pyridyl N43 in the molecule at $(1-x, -\frac{1}{2}+y, \frac{1}{2}-z)$, thus producing a $C(10)$ chain running parallel to the [010] direction and generated by the 2_1 screw axis along (0.5, *y*, 0.25) (Fig. 13). The same N2 atom also acts as a donor, *via* H2*B*, to pyridyl N63 in the molecule at $(-\frac{1}{2}+x, \frac{3}{2}-y, -z)$, producing another $C(10)$ chain, this time parallel to the [100] direction and generated by the 2_1 screw axis along (*x*, 0.75, 0) (Fig. 14). The combination of the two hydrogen bonds generates a third chain, of $C_2^2(20)$ type in which the two independent hydrogen bonds alternate, running parallel to the [001] direction. The amino N2 atom in the molecule at $(1-x, -\frac{1}{2}+y, \frac{1}{2}-z)$ acts as a donor, *via* H2*B*, to N63 in the molecule at $(\frac{3}{2}-x, 1-y, \frac{1}{2}+z)$; N2 at $(\frac{3}{2}-x, 1-y, \frac{1}{2}+z)$ in turn acts as a donor, *via* H2*A*, to N43 at $(\frac{1}{2}+x, \frac{3}{2}-y, 1-z)$; and N2 at $(\frac{1}{2}+x, \frac{3}{2}-y, 1-z)$ acts as a donor, *via* H2*B*, to N63 at $(x, y, 1+z)$ (Fig. 15).

The combination of these three chains, along [100], [010] and [001], is sufficient to generate the three-dimensional

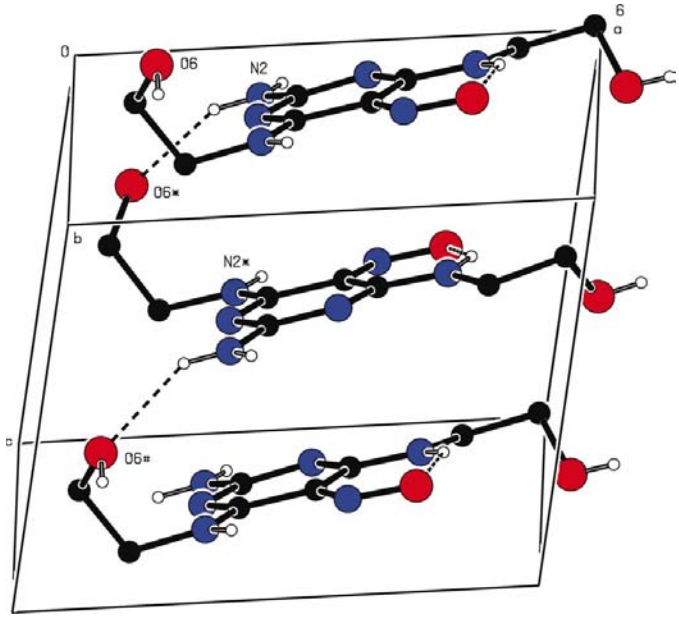

Figure 19
Part of the crystal structure of (6) showing the formation of a $C(9)$ chain along [001]. The atoms marked with an asterisk (*) or a hash (#) are at the symmetry positions $(x, \frac{1}{2}-y, \frac{1}{2}+z)$ and $(x, y, 1+z)$, respectively.

framework; this framework is, in fact, reinforced by both a C—H···π(arene) hydrogen bond (Table 3) and an aromatic $\pi\cdots\pi$ stacking interaction. The pyridyl C65 atom in the molecule at (x, y, z) acts as a hydrogen-bond donor to the pyridine ring (N63, C61–C66) in the molecule at $(-\frac{1}{2}+x, \frac{5}{2}-y, -z)$. These two molecules lie in adjacent [100] chains, offset by translation along the [010] direction: hence this C—H···π(arene) hydrogen bond links the [100] chains into a (001) sheet (Fig. 14). Finally, the pyrimidine ring in the molecule at (x, y, z) and the pyridine ring (N63, C61–C66) in the molecule at $(\frac{1}{2}+x, \frac{3}{2}-y, -z)$, both within the same [100] chain, are nearly parallel with an interplanar dihedral angle of only 5.3 (2)°, a centroid separation of 3.390 (2) Å and an interplanar spacing of *ca* 3.38 Å, and so modestly reinforces the formation of the [100] chain.

It is noteworthy that the 5-nitroso group in (5) does not participate in any type of hydrogen bond: this compound thus provides an exception to the generally observed behaviour of 4-amino-5-nitrosopyrimidines where the O and N atoms of the nitroso groups are usually important acceptors of hydrogen bonds, which indeed often dominate the supramolecular aggregation (Quesada, Marchal *et al.*, 2002; Melguizo *et al.*, 2003).

The structure of (6) (Fig. 16) is characterized by extensive disorder involving both the 2-hydroxyethylamino substituents, as well as the nitroso group. The discussion here of the supramolecular structure considers only the major orientation of each of the disordered fragments. There are four intermolecular hydrogen bonds, one each of O—H···O, O—H···N, N—H···O and N—H···N types, and together they generate a single three-dimensional framework, the formation of which is most simply analysed in terms of three one-dimensional sub-structures.

The hydroxyl O4 atom in the molecule at (x, y, z) acts as a hydrogen-bond donor to the ring atom N1 in the molecule at $(1+x, y, z)$, thus generating by translation a $C(9)$ chain running parallel to the [100] direction (Fig. 17).

The sub-structure parallel to [010] involves two types of hydrogen bond. Hydroxyl O6 in the molecule at (x, y, z) acts as a hydrogen-bond donor to nitroso O5 in the molecule at $(1-x, 1-y, -z)$, thus forming a centrosymmetric $R_2^2(18)$ ring, centred at (0.5, 0.5, 0) and characterized by a rather short O—H···O hydrogen bond (Table 3). Amino N2 in the molecule at (x, y, z) acts as a hydrogen-bond donor, *via* H2*A*, to the ring N3 atom in the molecule at $(1-x, -y, -z)$ forming the now-familiar centrosymmetric $R_2^2(8)$ ring containing paired N—H···N hydrogen bonds, centred here at (0.5, 0, 0). Propagation by inversion of these two hydrogen bonds thus generates a chain of alternating $R_2^2(8)$ and $R_2^2(18)$ rings, running parallel to the [010] direction (Fig. 18).

Finally, amino N2 in the molecule at (x, y, z) acts as a hydrogen-bond donor, *via* H2*B*, to hydroxyl O6 in the molecule at $(x, \frac{1}{2}-y, \frac{1}{2}+z)$, thus producing a second $C(9)$ chain, this time running parallel to the [001] direction and generated by the *c*-glide plane at $y = 0.25$ (Fig. 19). The combination of the [100], [010] and [001] chains generates the continuous three-dimensional framework.

4. Concluding comments

The differing manifestations, in (1)–(6), of a range of hard and soft hydrogen bonds, along with aromatic $\pi\cdots\pi$ stacking interactions in (5), are such that no two compounds within this series of very closely related pyrimidines exhibit the same types of direction-specific intermolecular interactions. Much effort continues to be expended in attempts to compute, using a variety of *ab initio*, semi-empirical and heuristic methods, the structures of simple molecular compounds (Lommerse *et al.*, 2000; Motherwell *et al.*, 2002). However, weak forces of the types manifest here, dependent upon molecular polarizability and polarization, are not easy to model computationally, as the detailed charge distribution within molecules not only influences the expression of the weak intermolecular forces, but in turn may itself depend in a subtle way on the detailed molecular environment. The variations in the supramolecular aggregation behaviour within an extended series of related compounds, such as those described here, provides a keen test of computational methods for crystal-structure prediction, and the accurate prediction of behaviour across such a series would generate real confidence in the efficacy of the predictive method employed.

X-ray data were collected at the EPSRC X-ray Crystallographic Service, University of Southampton, using a Nonius Kappa-CCD diffractometer. The authors thank the staff for all their help and advice. JNL thanks NCR Self Service, Dundee, for grants which have provided computing facilities for this work.

References

Allen, F. H., Kennard, O., Watson, D. G., Brammer, L., Orpen, A. G. & Taylor, R. (1987). *J. Chem. Soc. Perkin Trans. 2*, pp. S1–S19.
Batten, S. R. & Robson, R. (1998). *Angew. Chem. Int. Ed.* **37**, 1460–1494.
Boeyens, J. C. A. (1978). *J. Cryst. Mol. Struct.* **8**, 317–320.
Cremer, D. (1984). *Acta Cryst.* B**40**, 498–500.
Cremer, D. & Pople, J. A. (1975). *J. Am. Chem. Soc.* **97**, 1354–1358.
Desiraju, G. R. & Steiner, T. (1999). *The Weak Hydrogen Bond*, pp. 86–89. Oxford University Press.
Evans, D. G. & Boeyens, J. C. A. (1989). *Acta Cryst.* B**45**, 581–590.
Ferguson, G. (1999). *PRPKAPPA*. University of Guelph, Canada.
Flack, H. D. (1983). *Acta Cryst.* A**39**, 876–881.
Flack, H. D. & Bernardinelli, G. (2000). *J. Appl. Cryst.* **33**, 1143–1148.
Gilli, P., Bertolasi, V., Ferretti, V. & Gilli, G. (1994). *J. Am. Chem. Soc.* **116**, 909–915.
Glidewell, C., Low, J. N., Marchal, A., Melguizo, M. & Quesada, A. (2002). *Acta Cryst.* C**58**, o655–o657.
Glidewell, C., Low, J. N., Melguizo, M. & Quesada, A. (2003). *Acta Cryst.* C**59**, o9–o13.
Gordy, W. (1947). *J. Chem. Phys.* **15**, 305–310.
Kotelevskii, S. I. & Prezhdo, O. V. (2001). *Tetrahedron*, **57**, 5715–5729.
Lommerse, J. P. M., Motherwell, W. D. S., Ammon, H. L., Dunitz, J. D., Gavezzotti, A., Hofmann, D. W. M., Leusen, F. J. J., Mooij, W. T. M., Price, S. L., Schweizer, B., Schmidt, M. U., van Eijck, B. P., Verwer, P. & Williams, D. E. (2000). *Acta Cryst.* B**56**, 697–714.
Low, J. N., Quesada, A., Marchal, A., Melguizo, M., Nogueras, M. & Glidewell, C. (2002). *Acta Cryst.* C**58**, o289–o294.

Marchal, A., Melguizo, M., Nogueras, M., Sánchez, A. & Low, J. N. (2002). *Synlett.* pp. 255–258.
Melguizo, M., Quesada, A., Low, J. N. & Glidewell, C. (2003). *Acta Cryst.* B**59**, 263–276.
Motherwell, W. D. S., Ammon, H. L., Dunitz, J. D., Dryabchenko, A., Erk, P., Gavezzotti, A., Hofmann, D. W. M., Leusen, F. J. J., Lommerse, J. P. M., Mooij, W. T. M., Price, S. L., Scheraga, H., Schweizer, B., Schmidt, M. U., van Eijck, B. P., Verwer, P. & Williams, D. E. (2002). *Acta Cryst.* B**58**, 647–661.
Nonius (1997). *Kappa-CCD Server Software.* Windows 3.11 Version. Nonius BV, Delft, The Netherlands.
Otwinowski, Z. & Minor, W. (1997). *Methods Enzymol.* **276**, 307–326.
Quesada, A., Low, J. N., Melguizo, M., Nogueras, M. & Glidewell, C. (2002). *Acta Cryst.* C**58**, o355–o358.
Quesada, A., Marchal, A., Low, J. N. & Glidewell, C. (2003). *Acta Cryst.* C**59**, o102–o104.
Quesada, A., Marchal, A., Melguizo, M., Nogueras, M., Sánchez, A., Low, J. N., Cannon, D., Farrell, D. M. M. & Glidewell, C. (2002). *Acta Cryst.* B**58**, 300–315.
Schlemper, E. O., Murmann, R. K. & Hussain, M. S. (1986). *Acta Cryst.* C**42**, 1739–1743.
Sheldrick, G. M. (1997*a*). *SHELXL*97. University of Göttingen, Germany.
Sheldrick, G. M. (1997*b*). *SHELXS*97. University of Göttingen, Germany.
Spek, A. L. (2003). *J. Appl. Cryst.* **36**, 7–13.
Talberg, H. J. (1977). *Acta Chem. Scand. A*, **31**, 485–491.
Wilson, A. J. C. (1976). *Acta Cryst.* A**32**, 994–996.